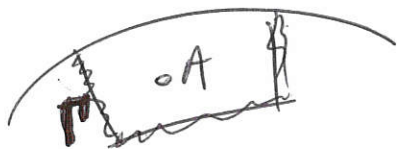


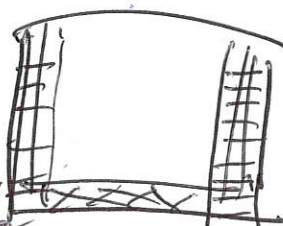
## Etape 1

Source A dans la  
boîte 3D Specfer  
autour de la source



Pout → Calculer  $\vec{u}$  et  $\vec{T}$  le long de P  
(donc boîte plus grosse et mettre  
PTCL)

Enregistrer  $\vec{u}$  et  $\vec{T}$



Differences with respect to

Nadine

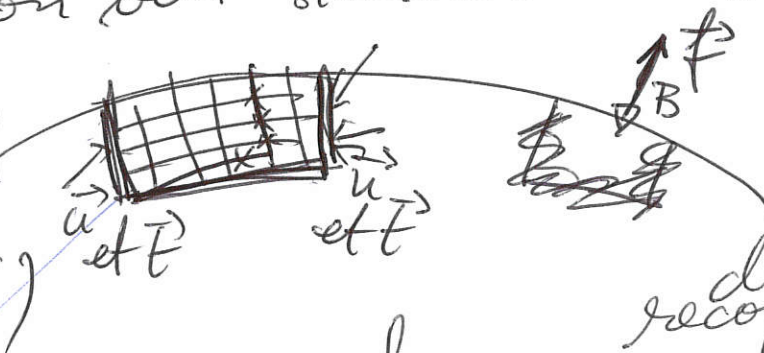
① il faut  $\vec{u}$  → donne champ  $U^{3D}$  et traction  $T^{3D}$

② il faut enregistrer sur un contour interne (bord interne des PTCLs?) au lieu du bord externe



Etape 2: Calculer une source B située  
à la position du récepteur (en surface),  
par exemple une force verticale  
si on veut simuler une source verticale)

call  
compute 3D  
want field using  
a nice cheap  
2D trick()



Differences  
① Change la source

② du coup changer la reconstitution de la vraie source

avec une force au lieu  
d'un CMT. On enregistre sans  
 $\vec{u}$  et  $\vec{T}$  sur les bords. force et non  
plus un CMT.

donne  $U^{1D}$  et traction  $T^{1D}$

### Étape 3:

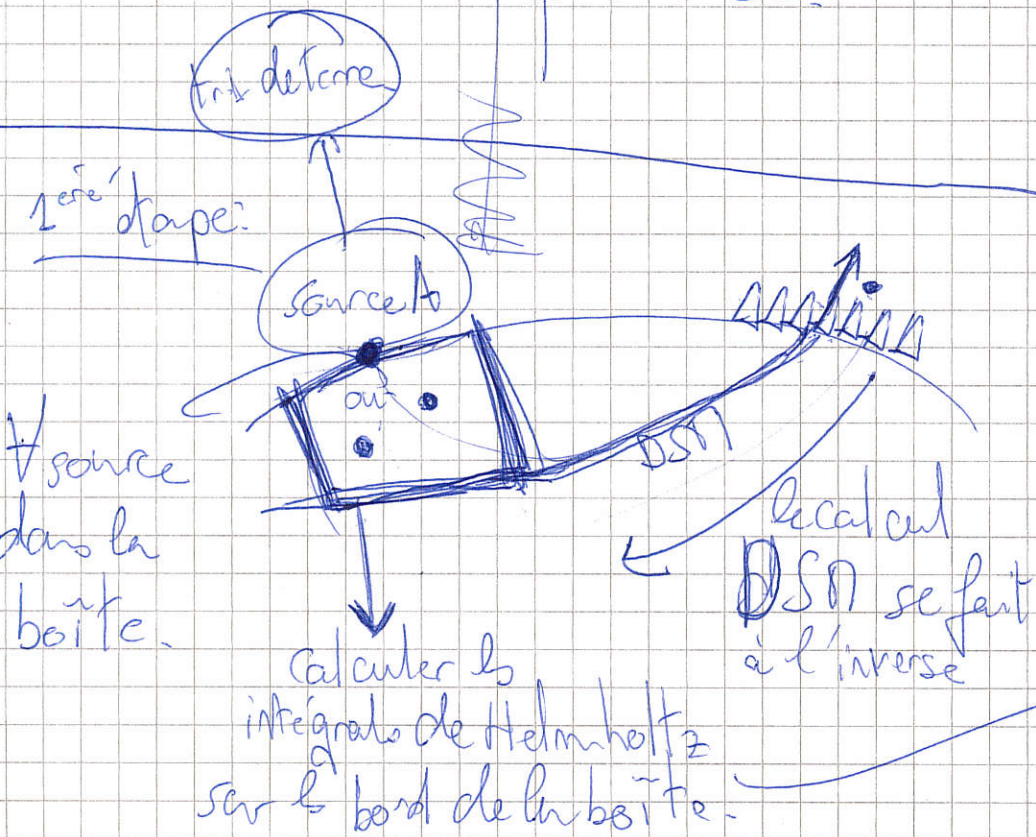
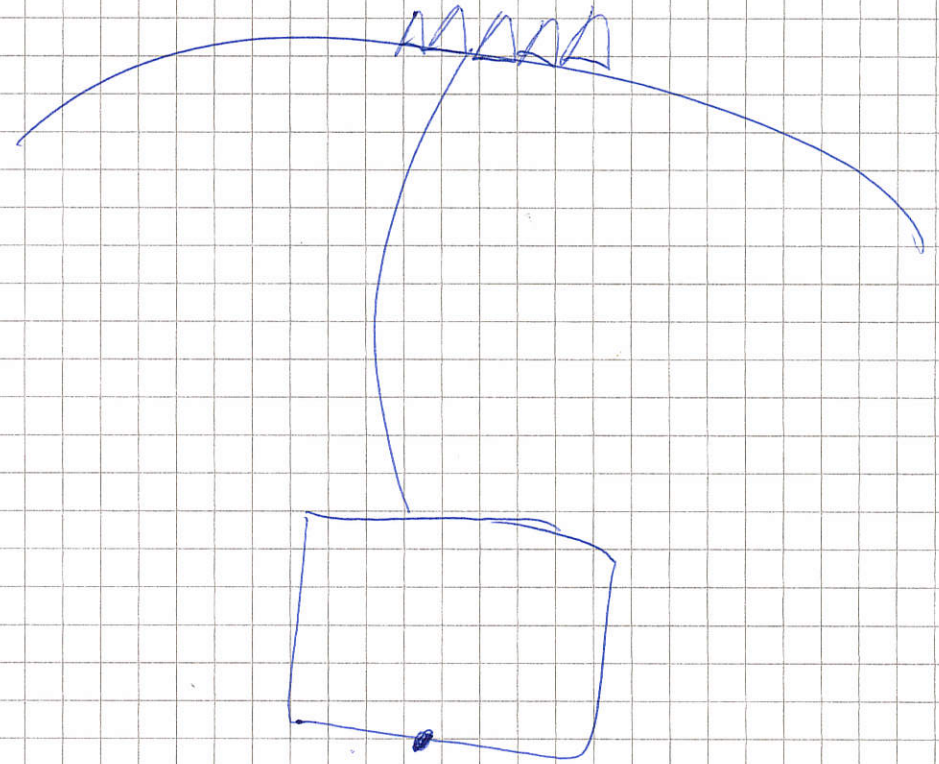
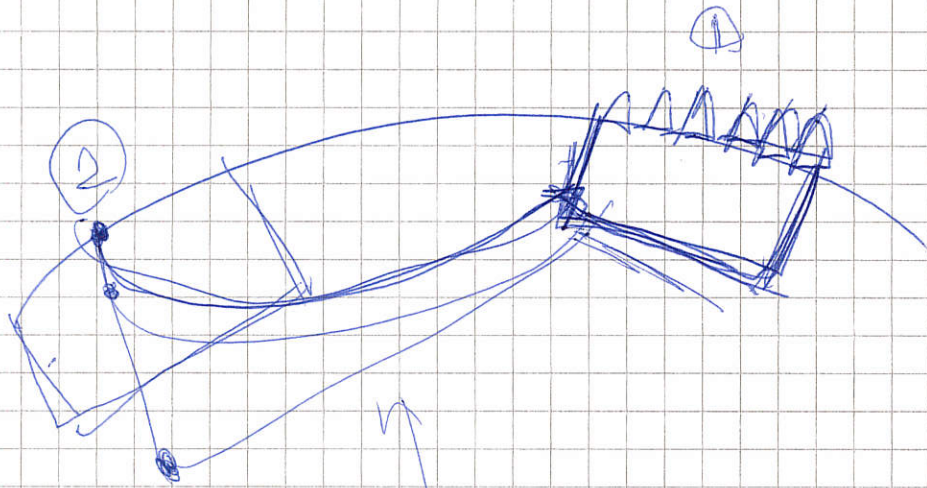
Intégrale de Hellmoltz

qui couple 1 et 2.

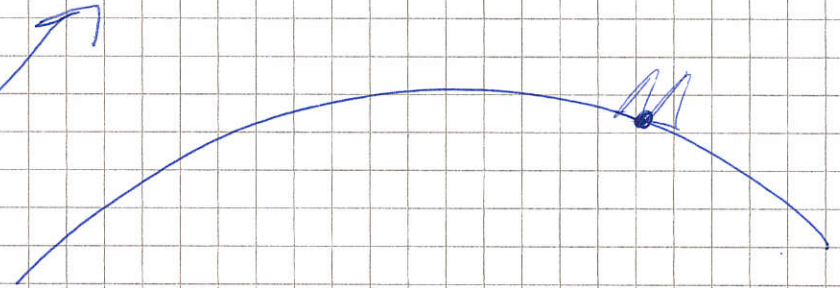
\* qui combine déplacement champ 1  
traction champ 2 - déplacement  
champ 2 traction champ 1.

① Coder une intégrale de GLL pour  
faire ça.



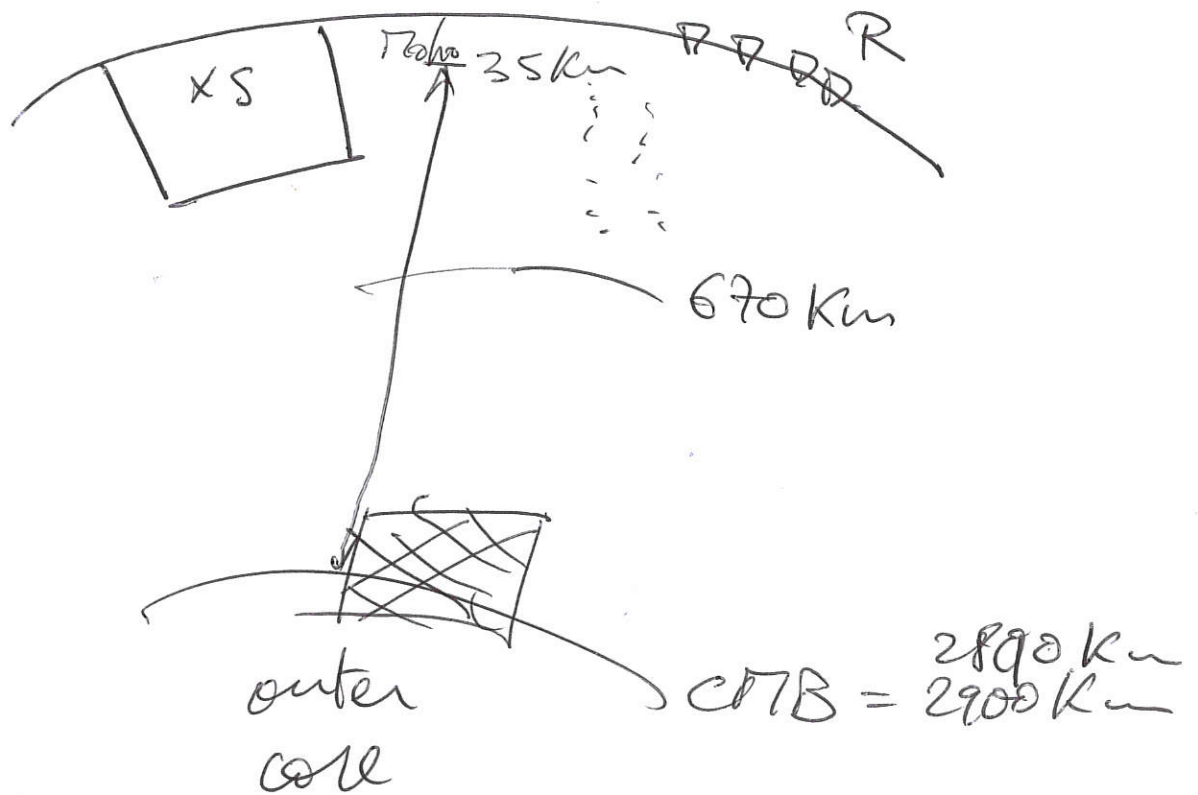


$$\int_S (\vec{u}^{3D} \cdot \vec{T}^{1D} - \vec{T}^{3D} \cdot \vec{u}^{1D}) dS$$

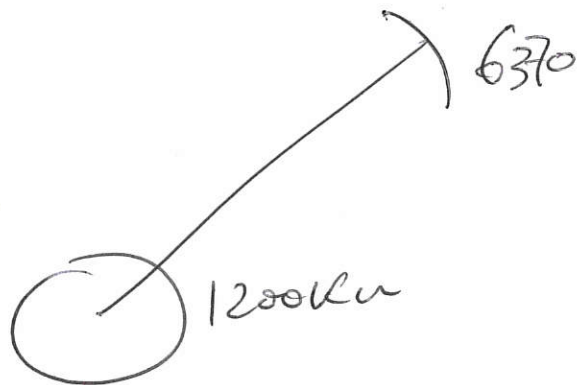


Cas d'une boîte située à la CTB :

(4)



Cas du inner core :



$$V = \left(\frac{1}{5}\right)^3 = \underline{\underline{1\%}}$$

# A SEMI-ANALYTIC-FEM HYBRID MODEL FOR SIMULATING UT CONFIGURATIONS INVOLVING COMPLICATED INTERACTIONS OF WAVES WITH DEFECTS

Nicolas Gengembre<sup>1</sup>, Alain Lhémy<sup>1</sup>, Ryuji Omote<sup>1</sup>,  
Thierry Fouquet<sup>2</sup> and Andreas Schumm<sup>2</sup>

<sup>1</sup>Commissariat à l'Énergie Atomique, LIST, CEA-Saclay, bât. 611, 91191 Gif-sur-Yvette cedex, France

<sup>2</sup>EDF/R&D/Sinetics, 1, avenue du Général De Gaulle, 92141 Clamart, France

**ABSTRACT.** A hybrid model is developed combining advantages of both semi-analytical and numerical methods. Most of the propagation is computed semi-analytically (pencil method, code Civa), while wave – defect interaction is computed numerically (FEM, code Athena) in a small region surrounding the defect. Both codes exchange results required to predict responses from defects through an integral formula extending Auld's principle to the transient case. The theory and its implementation are discussed. Examples illustrate its interest in UT simulations involving complicated interactions.

## INTRODUCTION

Semi-analytical models for UT simulation provide quantitative predictions in a wide range of situations. They allow fast computations, a crucial requirement in the industrial context. However, approximations made in deriving them may fail at predicting responses from defects of complex geometry where scattering involves complicated processes.

Numerical schemes such as FEM in computations of elastic wave phenomena do not rely on physical approximations. Numerical approximations are quantitatively well defined by theoretical considerations made in deriving the numerical formulation. However, numerical schemes are computer intensive (computation time, memory) considering typical wavepaths of hundreds of wavelengths in NDT configurations.

To combine the advantages of both methods while minimizing their inconveniences, a hybrid model has been developed. Most of the propagation is computed using a semi-analytical model (CEA, *Champ-Sons* model of *Civa*), while wave – defect interaction is computed numerically by a FEM scheme (EDF/INRIA code *Athéna*) in a small region surrounding the defect. An integral formulation extending Auld's reciprocity principle to the transient case has been derived to allow both codes to exchange the computed results required to predict the echo-response from the defect. In this paper, the theoretical derivation of the coupling formula is first derived. Then, its numerical implementation is discussed. Lastly, examples are given to illustrate the capabilities of hybrid computations in UT simulations.

## HYBRIDIZATION OF FEM AND SEMI-ANALYTICAL MODELS

In this part, the finite element model *Athéna* and the semi-analytical model *Champs* are shortly described. Then, the coupling formula to link them together is derived.

### *Athéna*, Finite Element Model for Wave Interaction with Complex Defects

The modeling code *Athéna* simulates wave propagation in heterogeneous and anisotropic media, in the presence of a complex shaped defect, solving the elastodynamic equations by a finite element method. The code emanates from a collaboration between INRIA and EDF [1]. The method chosen allies both the accuracy of finite elements and the performance of finite differences.

We recall the elastodynamic equations in their velocity  $\mathbf{v}$  / stress  $\mathbf{T}$  formulation :

$$\begin{cases} \rho \frac{\partial \mathbf{v}}{\partial t} - \text{div} \mathbf{T} = \mathbf{f} \\ \mathbf{A} \frac{\partial \mathbf{T}}{\partial t} - \boldsymbol{\varepsilon}(\mathbf{v}) = 0 \end{cases} \quad (1)$$

where  $\rho$  denotes the specific weight of the medium,  $\mathbf{A}$  the inverted Hooke's tensor,  $\boldsymbol{\varepsilon}(\mathbf{v})$  the displacement velocity tensor and  $\mathbf{f}$  the external forces. In the presence of a defect  $\Gamma$ , we add a third equation  $\mathbf{T} \cdot \mathbf{n} = \mathbf{0}$  on  $\Gamma$  where  $\mathbf{n}$  is the outward pointing normal on the defect.

The spatial discretization is done by mixed finite elements Q1-Q0 [2], which allows to use the condensation of the mass matrix and a regular mesh. Combined with an explicit scheme for the time discretization, we obtain a virtually explicit and therefore very fast resolution method.

Taking the defect into account requires imposing zero stress on the defect boundary, for which two methods are traditionally used. In both methods, the condition appears explicitly in the formulation. In the first one, one can revert to a structured (regular) mesh and approximate the defect geometry within the regular mesh (fig. 1-a), which can give rise to spurious diffraction. In the second one, an irregular mesh is adapted to the geometry (fig. 1-b), which is rather inconvenient for parametric studies, where each configuration requires a new mesh. Furthermore, the irregularity of the mesh with respect to the stability condition requires a very fine temporal discretization, and is thus more computation-intensive for a given precision.

The *Athéna* code therefore uses the fictitious domain method [3] as a different choice to represent the defect. In this method, a regular mesh is maintained and complemented by a discontinuous displacement over the defect as an additional unknown, defined over an additional mesh well adapted to the defect geometry (fig. 1-c). This

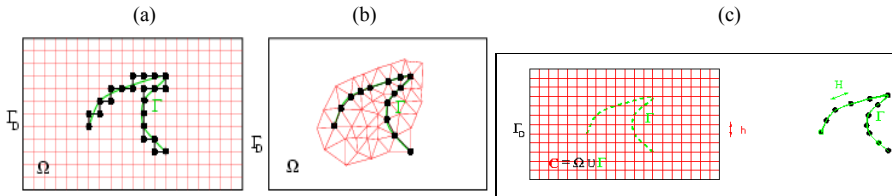


**FIGURE 1.** Different kinds of mesh for the defect in FEM. a- regular mesh. b- irregular mesh. c- fictitious domains.



approach requires the resolution of a new system of linear equations whose size depends on the resolution of the defect discretization. The ability of the method to handle a complex shaped defect within a regular mesh far outweighs this drawback.

### **The CIVA Semi-Analytical Model for Wave Propagation**

The semi-analytical model for field prediction *Champ-Sons* [4] implemented in the *Civa* software platform (see for example [5]) has been developed at CEA for about a decade. In this model, the calculation of the field radiated by an arbitrary transducer into a component is based on an extended form of Rayleigh integral, taking into account refractions and reflections at interfaces constituting the component to be tested. The particle displacement at point P  $u_p(t)$  is written as:

$$u_p(t) = V(t) \otimes \iint_{S \in \text{transducer}} G_{sp}(t) dS, \quad (2)$$

where  $G_{sp}(t)$  is the transient Green function for a point source S and an observation point P, and  $V(t)$  is the particle velocity perpendicular to the emitting surface. The elementary field  $G_{sp}(t)$  for each couple of points is evaluated analytically by means of the pencil method approximation. As explained for instance in Ref. 4, each elementary field  $G_{sp}(t)$  can be expressed by means of a time and an amplitude, that are evaluated along the geometrical ray path between S and P. The amplitude is evaluated using the divergence of a cone of rays (*i.e.* a pencil) surrounding the geometrical path. Its evolution depends on the media and interfaces crossed by the pencil, and is mathematically described by a product of matrices. This method allows to take into account anisotropic and heterogeneous components. Since the integration over the emitting surface is performed numerically (the surface being discretized into point sources), the transducers considered can also be arbitrarily shaped, including phased array transducers [6]. The resulting field can be expressed in terms of impulse responses, when  $V(t)$  is a Dirac  $\delta$ -function.

### **Derivation of the Coupling Formula**

The coupling of the two models *Champ-Sons* and *Athéna* aims at separating the computation of the propagation of a wave and its interaction with a defect. Therefore, one considers two different NDE configurations: the first one, called state 1, involves a sound component, whereas in the second one, called state 2, the component contains a flaw. The idea is that *Champ-Sons* and *Athéna* will be respectively devoted to the computation of

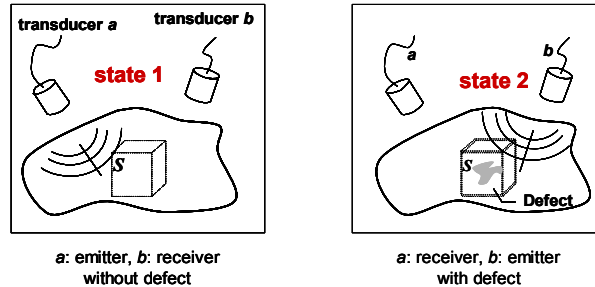


**FIGURE 2.** Definition of state 1 and state 2 in Auld's reciprocity principle.

state 1 and state 2.

In what follows, one derives a formula for linking the two states and obtaining the echo-response from the defect. This is performed using Auld's reciprocity principle [7]. Indeed, Auld establishes a relation between two typical NDT configurations, as defined in Figure 1: in state 1, two transducers a et b are involved to test a sound component, the transducer a being an emitter and the transducer b a receiver. In state 2, the component contains a flaw, transducer b is an emitter and transducer a is a receiver. Auld establishes that these two states can be linked by means of a surface integral allowing to express the difference between

- the transmission coefficient from transducer b to transducer a in the presence of defect,
- the transmission coefficient from transducer a to transducer b in the absence of defect.

This difference is expressed by  $\delta\Gamma_{ba}$  and writes:

$$\delta\Gamma_{ba}P = \frac{1}{4} \iint_S \left[ \mathbf{v}_i^{(1)} \cdot \mathbf{T}_{ij}^{(2)} - \mathbf{v}_i^{(2)} \cdot \mathbf{T}_{ij}^{(1)} \right] n_j dS, \quad (3)$$

where  $\mathbf{v}$  is the particle velocity,  $\mathbf{T}$  is the stress tensor,  $n d\mathbf{S}$  is a surface vector,  $S$  is the surface of integration surrounding the defect and  $P$  is the power provided to the emitter. Exponents (1) or (2) stand for the state considered.

In what follows, one will consider a pulse-echo configuration, *i.e.* transducer a and transducer b are just the same and  $\delta\Gamma_{ba}(t)$  becomes  $\delta\Gamma_{aa}(t)$ .

In Eq. 3, CW sources are assumed. In the present work, one aims at modeling wideband transducers, so that  $P$  and  $\delta\Gamma_{aa}$  are time-dependent. Thus, one needs to develop the transient formulation of this expression. For this, we use the property that states 1 and 2 can be taken at different times. Then, state 1 is evaluated at  $t_1 = \tau$  and state 2 at  $t_2 = t - \tau$ . After performing an integration over  $\tau$  in both sides of Eq. 3, convolution products (denoted as  $*$ ) appear, and one gets:

$$\delta\Gamma_{aa}(t) * P(t) = \frac{1}{4} \iint_S \left[ \mathbf{v}_i^{(1)}(\tau) \cdot \mathbf{T}_{ij}^{(2)}(t - \tau) - \mathbf{v}_i^{(2)}(t - \tau) \cdot \mathbf{T}_{ij}^{(1)}(\tau) \right] n_j dS d\tau \quad (4)$$

Since the quantity to be computed is  $\delta\Gamma_{aa}(t)$ , one needs to perform a symbolic deconvolution with  $P(t)$ , that is the transient excitation signal. This means that impulse responses will appear in the integral instead of convolved signals. For each of the two products involved inside the integral, deconvolution can be applied to either stresses or velocities, so that four different formulations can be written, and two impulse responses appear. Since *Civa* is well adapted to the computation of impulse responses, whereas *Athéna*, like any FEM model, would require the computation of very high frequencies, thus the use of very small meshes, the best solution among the four possible ones writes:

$$\delta\Gamma_{aa}(t) = \frac{1}{4} \iint_S \left[ h \mathbf{v}_i^{(1)}(t) * \mathbf{T}_{ij}^{(2)}(t) - \mathbf{v}_i^{(2)}(t) * H \mathbf{T}_{ij}^{(1)}(t) \right] n_j dS, \quad (5)$$

so that the impulse responses  $h \mathbf{v}_i^{(1)}$  and  $H \mathbf{T}_{ij}^{(1)}(t)$  (respectively for velocities and stresses) are given by *Champ-Sons*.



This latter equation gives then difference between the two states, that is the echo-response from the defect.

## NUMERICAL IMPLEMENTATION

The hybrid model coupling *Champ-Sons* and *Athéna* has been implemented within the *Civa* software platform. In this part, we aim at describing how the states 1 and 2, involved in the coupling formula (Eq. 5), are effectively computed.

The region in which the FEM computation is used must be as small as possible, in order to avoid intensive computation. Then state 2 is only considered inside the surface *S* surrounding the defect, called FEM box. This box is a rectangle for 2D computations and a parallelepiped for 3D computations. On one face of the box, the incident field, expressed by the three components of the force, is computed by means of *Champ-Sons*. This field is then used as a source in *Athéna* computation. This *input face* must be the first face crossed by the incident beam. Moreover, the input face must be located far enough from the defect, to ensure that no reflected echo can reach this face before the emission is finished. Indeed, a point in the FEM scheme cannot be simultaneously a source and a receiver.

The limitation of the source term due to the lateral size of the input face may lead to aperture diffraction effects, which would lead to artificial diffracted edge waves. To avoid this, an apodization function is applied to the source term so that it decreases smoothly to zero at the edges.

*Athéna* requires two distinct meshes. For 3D computations, a regular cubic mesh is required for the volume, without account of defects. The defect is a surface that is meshed separately. In 2D computations, a 2D rectangle regularly meshed and a linear mesh for the defect are required. The boundary conditions applying on the different faces of the box are perfectly absorbing conditions, so that no artificial reflection arises from these faces.

Once the computation is performed, results are available for all the points belonging to the main mesh, but only those belonging to the surrounding surface are required for the computation of the coupling formula. At these points, the field corresponding to state 1 is computed by means of *Champ-Sons* in terms of impulse responses, for particle velocities and stresses. The coupling integral formula can then be computed. The resulting signal is the A-scan obtained in the presence of the defect in the configuration considered.

The first computations made using the hybrid model have shown the presence of an artifact in the echo-response, due to an artificial reflection on the input face of the FEM box. Anyhow, if the dimensions of the box and the discretization are properly defined, the amplitude of this numerical noise is very low. Moreover, it is easily filtered since its time and duration are known, and no real echoes from defect can appear at these time-of-flights.

## RESULTS

### **Diffraction of a T45 Beam by a Vertical Crack**

The coupling method has been applied to the computation of the echo arising from a vertical crack. This crack is 15mm height and the ultrasonic beam is generated by a T45° 2MHz transducer (see Fig. 3-a)

The result predicted by the hybrid model is given in figure 3-c. In the resulting signal, four main echoes have been predicted. Echo number 1 corresponds to the near tip diffraction echo, echo number 2 is the far tip diffraction echo, and the two other echoes are due to Rayleigh surface waves. Indeed, in this configuration, Rayleigh waves are generated at one of the tips, propagate along the crack and are then converted into bulk waves at the other tip. This leads to the echo number 3, predicted by the hybrid model. Moreover, a

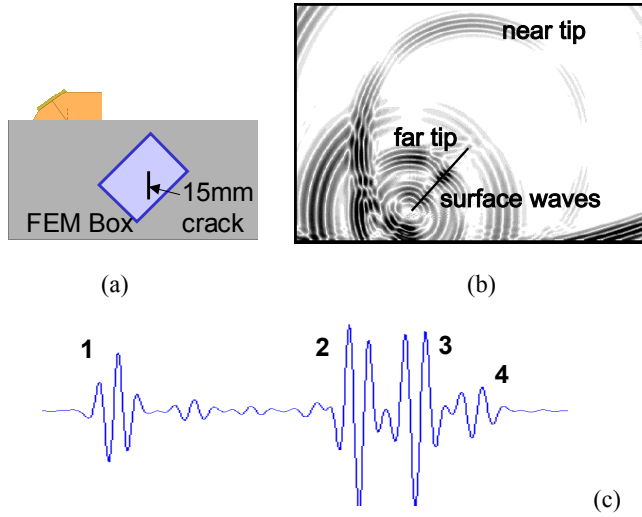


**FIGURE 3.** a- Configuration used for the computation of echoes coming from a vertical crack in a T45 test. b- Snapshot obtained inside the FEM box after beam/defect interaction. c- A-scan predicted by the hybrid model in this configuration.

certain amount of the Rayleigh wave is not converted into bulk wave, but reflected, so that the surface wave propagates twice along the crack. This leads to echo number 4. Figure 3-b shows a snapshot after wave defect interaction obtained inside the FEM box, where the different echoes are emphasized. These results can be compared with the results obtained by means of a transient GTD approach, developed in Ref. 8 aiming at taking the surface wave into account. For the same configuration, the amplitudes of the different echoes are similar for both methods. The method developed in Ref. 8 is limited to simple configurations (planar cracks) whereas the hybrid model allows to predict the response of defects of complex geometry, as illustrated by the next example.

#### **Diffraction of a T45 Beam by a Vertical Irregular Crack**

The interaction of a beam with an irregular crack is now studied. The transducer is the same as in the previous example, and the tips of the irregular crack coincide with those in the previous example. The shape of the crack is described in figure 4-a.

In figure 4-c, the resulting A-scan is presented and compared with that predicted

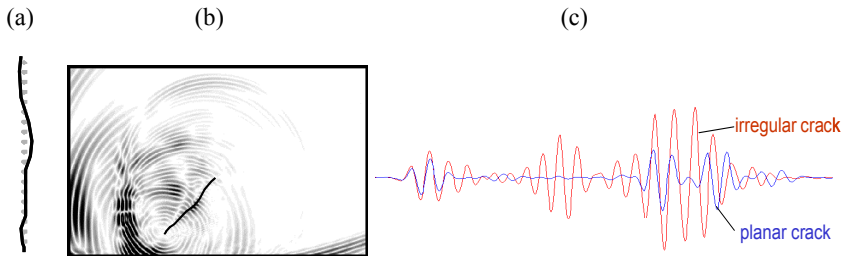


**FIGURE 4.** a- Crack profile. b- Snapshot obtained in the FEM box after interaction of the beam with the irregular crack. c- A-scan predicted by the hybrid model in presence of the irregular crack.

with a planar crack. Echoes from the near tip in both configurations are nearly the same, whereas the one from the far tip is of higher amplitude in the irregular case than in the regular one.

The echo due to the propagation of surface waves along the crack can hardly be distinguished from the far tip diffraction echo in the response of the irregular crack. Moreover, an echo appears between the two diffraction echoes. The snapshot representation (figure 4-b) shows that this contribution comes from a bump in the crack profile.

## CONCLUSIONS AND PERSPECTIVES

A method for coupling a finite element code and a semi-analytical model has been developed. It is based on a transient form of Auld's reciprocity principle, in which the results of both models are linked together through a surface integral surrounding the defect (or a contour integral for 2D computations). Based on this method, a hybrid model coupling the FEM code *Athéna* for beam-defect interaction and the semi-analytical model *Champs* for field computation has been implemented within the *Civa* software platform. Examples of predictions made using this hybrid model have been presented showing the capabilities of this approach.

Further developments of *Athéna* are now in progress in order to deal with multiple defects, partially closed cracks, and local mesh refinement to improve its ability to handle geometry details or singularities. The use of the hybrid model will then enable to compute echo responses of complex defects in various NDT configurations.

## REFERENCES

1. Tsogka, C., "Modélisation mathématique et numérique de la propagation des ondes élastiques tridimensionnelles dans les milieux fissurés », Ph.D. thesis, University Paris IX, 1999.
2. Bécache, E., Joly, P., Tsogka, C., *SIAM J. Numer. Anal.* **37**, 1053-1084 (2000).
3. Bécache, E., Joly, P., Tsogka, C., *J. Comput. Acoust.* **9**, 1175-1202 (2001).
4. Gengembre, N. and Lhémy, A., "Calculation of wideband ultrasonic fields radiated by water-coupled transducers into heterogeneous and anisotropic media", in *Review of progress in QNDE*, Vol. 19, edited by D. O. Thompson and D. E. Chimenti, AIP Conference Proceedings 509, Melville, New-York, 2000, pp. 977-984.
5. Benoist, Ph., Besnard, R., Bayon, G. and Boutaine, J.-L., "Civa workstation for NDE: mixing of NDE techniques and modeling", in *Review of Progress in QNDE*, Vol. 14, edited by D. O. Thompson and D. E. Chimenti, Plenum, New-York, 1995, pp. 2353-2360.
6. Mahaut S., Calmon P., Chatillon S. and Raillon R., "Ultrasonic NDT simulation tools for phased array techniques", in *Review of progress in QNDE*, Vol. 22, edited by D. O. Thompson and D. E. Chimenti, AIP Conference Proceedings 509, Melville, New-York, 2002, pp. 777-784.
7. Auld, B. A., *Wave motion* **1**, 3-10 (1979).
8. Butin, L. and Lhémy, A., "A transient model for the simulation of ultrasonic nondestructive experiments including surface wave effects on cracks", in *Review of Progress in QNDE*, Vol. 18, edited by D. O. Thompson and D. E. Chimenti, Plenum, New-York, 1999, pp. 135-142.